Dynamics of Atmospheres and Oceans 73 (2016) 87–97

Contents lists available at ScienceDirect

Dynamics of Atmospheres and Oceans

journal homepage: www.elsevier.com/locate/dynatmoce

New layer thickness parameterization of diffusive convection in the ocean

Sheng-Qi Zhou [a,*], Yuan-Zheng Lu [a,b], Xue-Long Song [a,c], Ilker Fer [d]

[a] State Key Laboratory of Tropical Oceanography, South China Sea Institute of Oceanology, 164 West Xingang Road, Haizhu District, Guangzhou 510301, China
[b] University of Chinese Academy of Sciences, Beijing 100101, China
[c] School of Marine Information Engineering, Guilin University of Electronic Technology, Beihai 536000, China
[d] Geophysical Institute, University of Bergen, Bergen, Norway

ARTICLE INFO

Article history:
Received 17 April 2015
Received in revised form 9 December 2015
Accepted 5 January 2016
Available online 28 January 2016

Keywords:
Diffusive convection
Convecting layer thickness
Parameterization

ABSTRACT

In the present study, a new parameterization is proposed to describe the convecting layer thickness in diffusive convection. By using in situ observational data of diffusive convection in the lakes and oceans, a wide range of stratification and buoyancy flux is obtained, where the buoyancy frequency N varies between 10^{-4} and 0.1 s^{-1} and the heat-related buoyancy flux q_T varies between 10^{-12} and 10^{-7} $m^2\,s^{-3}$. We construct an intrinsic thickness scale, $H_0 = [q_T^3/(\kappa_T N^8)]^{1/4}$, here κ_T is the thermal diffusivity. H_0 is suggested to be the scale of an energy-containing eddy and it can be alternatively represented as $H_0 = \eta Re_b Pr^{1/4}$, here η is the dissipation length scale, Re_b is the buoyant Reynolds number, and Pr is the Prandtl number. It is found that the convective layer thickness H is directly linked to the stability ratio R_ρ and H_0 with the form of $H \sim (R_\rho - 1)^2 H_0$. The layer thickness can be explained by the convective instability mechanism. To each convective layer, its thickness H reaches a stable value when its thermal boundary layer develops to be a new convecting layer.

1. Introduction

Double-diffusion is one of the most important non-mechanically driven mixing processes. Its importance has been particular recognized in oceanography (Schmitt, 1994), material science (Langlois, 1985), geology (Robb, 2004), and planetary physics (Chabrier and Baraffe, 2007). In oceans, about 44% regions display double-diffusive process (You, 2002). In certain regions, e.g., the North Atlantic, the double-diffusive mixing is several times stronger than the turbulence mixing (Schmitt et al., 2005). Globally, the double-diffusive mixing alters the meridional overturning rate by 20% (Zhang et al., 1999).

Double-diffusion occurs in a fluid in which there are gradients of two (or more) properties with different molecular diffusivities and of opposing effects on the vertical density distribution. It has two primary modes: salt finger (SF) and diffusive convection (DC). Diffusive convection forms when cold and fresh water lies on top of warm and salty water. It is characterized by a series of thermohaline staircases where a stack of homogenous layers of nearly-constant temperature and salinity are separated by thin, strongly stratified interfaces (Kelley et al., 2003). An example of diffusive convection is shown in Fig. 1a.

* Corresponding author.
E-mail address: sqzhou@scsio.ac.cn (S.-Q. Zhou).

http://dx.doi.org/10.1016/j.dynatmoce.2016.01.001
0377-0265/

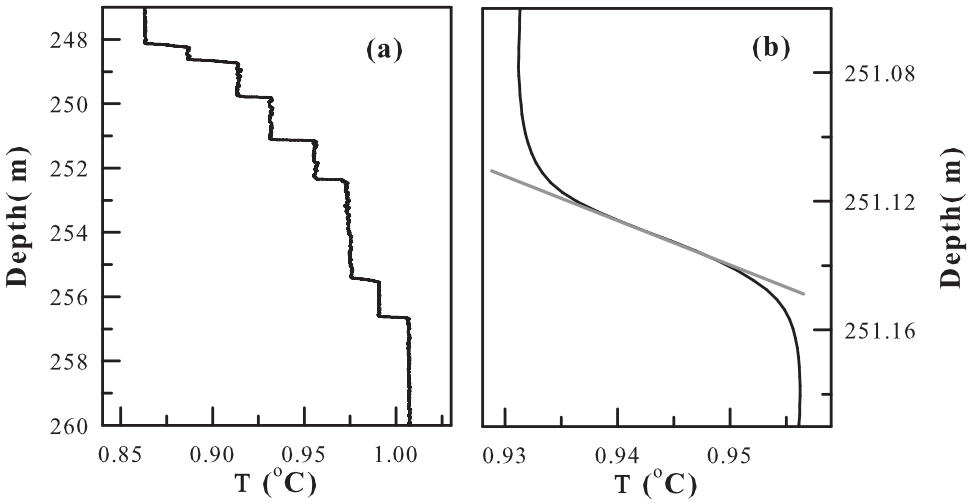

Fig. 1. (a) Typical diffusive convection staircases in the potential temperature profile measured by the Microstructure Profiler at (88.27° N, 0.53° E) in the Amundsen Basin in April 2008. (b) An example of DC interface, which is the zoom-in potential temperature profile in the depth range of 251.06–251.19 m. The gray line is a fitting line of the maximum slope inside the interface.

Recently, the importance of diffusive convection has aroused more interest due to its impact to the diapycnal mixing in interior ocean and the ice-melting in the Arctic and Antarctic Oceans (Turner, 2010; Wong and Riser, 2011; Sirevaag and Fer, 2012; Guthrie et al., 2015). However, the basic characteristics of diffusive convection cannot be well quantified by the available theoretical frames. One of them is the thickness of diffusive-convective layers, H. Since each convecting layer is bounded by two free neighboring interfaces, which quantities govern the thickness H is a key issue of concern. As the thickness is the basic element in the descriptions of flow dynamics and heat/salinity transport in the convecting layer, its accurate expression is needed to well evaluate the impact of diffusive convection in the oceans.

Some effort has been made to formulate it in previous investigations (Huppert and Linden, 1979; Kelley, 1984; Kerpel et al., 1991; Fedorov, 1988; Fernando, 1989). Among them, the parameterization proposed by Kelley (1984) seems popular to oceanographers. There are two main reasons why this particular parameterization has been extensively applied to describe the in situ diffusive convection staircases, e.g., in the Arctic Ocean (Timmermans et al., 2003; Turner, 2010; Sirevaag and Fer, 2012), and lakes (Rohden et al., 2010). One is that it shows reasonable agreement with the observations in various oceans and lakes (Kelley, 1984). The other one is that only the measurable properties are involved in the parameterization. However, as reported in Kelley et al. (2003) and Timmermans et al. (2003), the parameterization disagrees significantly with the observations, e.g., the predicted value is five times smaller than the observation in the deep Arctic Ocean (Timmermans et al., 2003). Additional effort is needed to elucidate the discrepancy.

It is worthy reviewing these existing parameterizations. In terms of the involved quantities, there are two main classes as follows.

1.1. Scaled by $(\kappa_T/N)^{1/2}$

In a laboratory experiment and the corresponding theoretical simulation, Huppert and Linden (1979) studied diffusive convection in a salt-stratified fluid heated from below. They proposed that the layer thickness (except the lowest layer) has the form of

$$H = 51\left(\frac{\kappa_T}{N'_S}\right)^{1/2}, \tag{1}$$

here κ_T is the thermal diffusivity and $N'_S = (g\beta(dS/dz))^{1/2}$ is the buoyancy frequency based on the initial salinity gradient, (dS/dz), with g and β being the gravitational acceleration and the haline contraction coefficient. This equation means that the average layer thickness depends only on the initial salinity gradient and fluid properties, and is therefore independent of the heat flux. In a subsequent laboratory experiment, a similar result was obtained except that the salinity diffusivity, κ_S, not the thermal diffusivity, κ_T, is more relevant to the layer thickness, H (Kerpel et al., 1991).

The thickness of diffusive convecting layers in the ocean was first taken up by Kelley (1984). He assumed that the length of diffusive convection is not determined by external factors, *e.g.*, internal wave or large-scale shearing. With dimensional analysis, he proposed that the combination of molecular properties of fluid and its fluid state can lead to an intrinsic length scale $H_0 = (\kappa_T/N)^{1/2}$, $N = (g\alpha(dT/dz) - g\beta(dS/dz))^{1/2}$ is the smoothed buoyancy frequency over the diffusive convection

staircases, where α is thermal expansion coefficient and (dT/dz) is the temperature gradient. Then, the layer thickness H was given by

$$H = G_1(Pr, R_\rho)\left(\frac{\kappa_T}{N}\right)^{1/2}, \tag{2}$$

where $G_1(Pr, R_\rho)$ is expressed as $G_1(Pr, R_\rho) = [2.5 \times 10^8 Pr R_\rho^{1.1}(R_\rho - 1)]^{1/4}$. Pr ($Pr = \nu/\kappa_T$) is the Prandtl number, where ν is the kinematic viscosity of the fluid. R_ρ ($R_\rho = \beta\Delta S/\alpha\Delta T$) is the stability ratio defined in terms of the buoyancy jumps across the convecting layer due to salinity (ΔS) and temperature (ΔT) variances. In the parameterization, it was proposed that the scaling of Eq. (2) holds because the thickness H is controlled by a balance between mixed-layer merging and interface splitting, whereby new layers are formed from the existing interfaces.

Fedorov (1988) extended the work of Kelley (1984) and proposed a similar expression of

$$H = G_2(Pr, R_\rho)\left(\frac{\kappa_T}{N}\right)^{1/2}, \tag{3}$$

where $G_2(Pr, R_\rho) = 0.91 Pr\, exp\{4.6\, exp[-0.54(R_\rho - 1)]\}$ is deduced from an empirical expression of Marmorino and Caldwell (1976). In Fedorov's work, $(\kappa_T/N)^{1/2}$ is a definite physical quantity, related to the thickness of the large gradient diffusive interface.

1.2. Scaled by $(q/N^3)^{1/2}$

An alternative class was developed by Fernando (1987, 1989). He suggested that the thickness H is determined by a balance between the kinetic and potential energies of turbulent eddies within the convecting layers (Fernando, 1987). Based on his laboratory work, where the salt-stratified fluid was heated from below, he proposed that the thickness of the bottom convecting layer is given by

$$H_b = 41.5\left(\frac{q_T}{N_S'^3}\right)^{1/2}, \tag{4}$$

here q_T is the buoyancy flux defined on the basis of the bottom heat flux F_T, a reference stable ρ_0, and the specific heat c_p as $q_T = g\alpha F_T/\rho_0 c_p$. This laboratory result was extrapolated for oceanic situation by Fernando (1989), which was in the form of

$$H = G_3(R_\rho)\left(\frac{q_T}{N_S^3}\right)^{1/2}, \quad R_\rho \ll 10, \tag{5}$$

here $G_3(R_\rho) = 14(1 - R_\rho^{-1})^{-3/4}$. In this parameterization, q_T is the instantaneous heat-related buoyancy flux of the convecting layer, and N_S is the buoyancy frequency based only on salinity stratification. Eq. (5) was further suggested to be valid only when diffusive convection is in the "quasi-stationary"state. This parameterization is less applicable because the buoyancy flux q_T cannot be measured directly by the current techniques, and some parameterizations for calculating q_T also depend on the thickness H (Fernando, 1989; Kelley, 1990). However, this model clearly indicates that the layer thickness H also depends on the heat-related buoyancy flux q_T.

In general, these models are all partially successful in predicting the thickness of convecting layer H. Up to now, little effort has been made to examine the inferences of them or to develop a new one to better represent the layer thickness. In the present work, a new parameterization is proposed to describe the thickness of convecting layer by constructing a new intrinsic thickness scale. Using available in situ observational data that cover wider ranges of heat-related buoyancy flux and stratification, we examine the applicability of the new parameterization by comparing it with the previous schemes. Moreover, the physics represented in the new parameterization is discussed in the classical frame of double-diffusive convection.

2. The new model

In the laboratory experiment of salt-stratified fluid, a series of convecting layers was progressively formed from below as the bottom being heated (Turner, 1968; Huppert and Linden, 1979; Fernando, 1987). Turner (1968) proposed the bottom convecting layer has a stable thickness as,

$$H_b = \left(\frac{1}{4}Ra_c Pr\right)^{1/4}\left(\frac{{q_0}^3}{\kappa_T N_S'^8}\right)^{1/4}, \tag{6}$$

where Ra_c is the critical Rayleigh number in diffusive convection. In his argument, it was suggested the bottom convecting layer gets thicker until its top boundary develops a new convecting layer triggered by the thermal instability. In Eq. (6), Ra_c and Pr are dimensionless and the expression of $(q_0^3/\kappa_T N_S'^8)^{1/4}$ offers a dimension scale. In the new model, we propose that the effects of buoyancy flux, thermal diffusion, and stratification should be included. As $(q_0^3/\kappa_T N_S'^8)^{1/4}$ includes all components,

we would make use of it as an intrinsic length scale H_0. In Eq. (6), q_0 is the buoyancy flux based on the bottom heat flux and N'_S is the buoyancy frequency of the initial condition. In the oceans or lakes, the background conditions of diffusive convection are not well-controlled as those in the laboratory. Thus, to each convecting layer, its heat buoyancy flux q_T and the oceanic background stratification N are alternatively used. Accordingly, the layer thickness H is proposed in the form of

$$H = G_4 H_0 = G_4(R_\rho)\left(\frac{q_T^3}{\kappa_T N^8}\right)^{1/4}, \tag{7}$$

where $G_4(R_\rho)$ is a function of R_ρ to be determined from the available in situ observations. Here Prandtl number Pr is not included in the function G_4 because it varies less (4–14) compared to other quantities, as listed in Table 1.

The heat buoyancy flux q_T of individual convecting layer can be obtained from the heat flux, F_T. However, same as the problems encountered in the parameterization of Fernando (1989), the in situ measurement of F_T in diffusive convection is nearly an impossible task. Several parameterizations were developed to evaluate the F_T of diffusive convection by using the experimental data in the laboratory (Marmorino and Caldwell, 1976; Taylor, 1988; Fernando, 1989; Kelley, 1990). All these parameterizations followed the spirit of Turner's (1973) work. It was suggested that the heat flux of diffusive convection be analogous to that in the Rayleigh–Bénard convection (Turner, 1973). In Rayleigh–Bénard convection, when it is assumed that the heat flux through a convecting layer is independent of the layer thickness H, the dimensional analysis yields a flux law of the form (Chandrasekhar, 1961; Siggia, 1994),

$$Nu \sim Ra^{1/3}, \tag{8}$$

where the Nusselt number, Nu, is the ratio of the convective flux to the conductive flux, while Rayleigh number, Ra, is the ratio of buoyancy force to diffusion. Both are defined as $Nu = F_T/(\kappa_T \rho c_p \Delta T/H)$ and $Ra = \alpha g \Delta T H^3/(\nu \kappa_T)$. Based on the recent precise laboratory measurements, it was suggested that the scaling of 1/3 in Eq. (8) holds well till $Ra < 5 \times 10^{14}$ (Brown et al., 2005; Nikolaenko et al., 2005; He et al., 2012). Equivalently, Eq. (8) can be written as

$$F_T = C\rho c_p \left(\frac{\alpha g \kappa_T^2}{\nu}\right)^{1/3} (\Delta T)^{4/3}, \tag{9}$$

where C is a constant of proportionality in thermal convection. Eq. (9) is called "4/3 flux law" (Turner, 1973). In the diffusive convection, C becomes a function of density ratio R_ρ. Some heat flux parameterizations are commonly used, which are in the forms of

$$C_M = 0.00859 \exp\{4.6 \exp[-0.54(R_\rho - 1)]\}, \tag{10a}$$

$$C_T = 0.272 R_\rho^{-0.21}, \tag{10b}$$

and

$$C_K = 0.0032 \exp((4.8/R_\rho^{0.72})), \tag{10c}$$

where the subscripts M, T, and K represent the heat flux formulas proposed by Marmorino and Caldwell (1976), Taylor (1988), and Kelley (1990), respectively. The corresponding heat buoyancy fluxes are denoted as q_{TM}, q_{TT}, and q_{TK}, respectively.

Table 1
Statistics of diffusive convection staircases. The averaging values are listed when more than one step is observed in data source. Data Sources: A – Zhou and Lu (2013); B – BGOS (2012); C – Neshyba et al. (1971); D – Perkin and Lewis (1984); E – Middleton and Foster (1980); F – Muench et al. (1990); G – Shirtcliffe and Calhaem (1968); H – Anschutz and Blanc (1996); I – Swift et al. (2012); J – Larson and Gregg (1983); K – Newman (1976); and L – Schmid et al. (2010).

Location	ΔT (°C)	H (m)	Pr	N(s^{-1})	N_S (s^{-1})	$R\rho$	q_{TM} ($m^2\ s^{-3}$)	q_{TT} ($m^2\ s^{-3}$)	q_{TK} ($m^2\ s^{-3}$)	*Source*
Arctic										
Deep	1.2×10^{-3}	46.4	13.3	2.3×10^{-4}	3.1×10^{-4}	3.1	1.6×10^{-12}	1.0×10^{-12}	1.0×10^{-12}	A
Upper 1	4.4×10^{-2}	3.1	13.3	5.0×10^{-3}	5.6×10^{-3}	4.7	2.9×10^{-11}	1.9×10^{-11}	3.0×10^{-11}	B
Upper 2*	2.3×10^{-2}	3.3	13.0	4.7×10^{-3}	4.9×10^{-3}	6.5	6.5×10^{-12}	3.2×10^{-12}	6.6×10^{-12}	C
Alpha ridge*	2.46×10^{-2}	2.1	13.6	5.9×10^{-3}	6.3×10^{-3}	6.9	7.8×10^{-12}	4.2×10^{-12}	7.6×10^{-12}	D
Antarctica										
Weddell Sea 1*	5.6×10^{-2}	3.2	13.4	1.4×10^{-3}	4.7×10^{-3}	1.6	4.4×10^{-10}	1.8×10^{-10}	1.8×10^{-10}	E
Weddell Sea 2†	7.8×10^{-2}	42.5	13.1	1.3×10^{-3}	2.6×10^{-3}	1.4	1.5×10^{-9}	5.7×10^{-10}	5.9×10^{-10}	F
Lake Vanda*,†	0.52	1.3	10.1	3.3×10^{-2}	3.6×10^{-2}	7.9	7.2×10^{-10}	3.9×10^{-10}	6.1×10^{-10}	G
Red Sea										
Atlantic II 1	4.08	19.7	3.8	0.13	0.14	12.0	1.8×10^{-7}	4.1×10^{-8}	1.6×10^{-7}	H
Atlantic II 2	4.43	10.1	4.3	0.17	0.17	12.5	1.9×10^{-7}	3.7×10^{-8}	1.6×10^{-7}	I
Bahamas*	4.7×10^{-2}	0.53	6.4	1.1×10^{-2}	1.8×10^{-2}	1.5	5.7×10^{-9}	2.3×10^{-9}	2.3×10^{-9}	J
Lake Kivu 1*,†	1.5×10^{-2}	1.1	6.0	6.0×10^{-3}	–	1.8	1.1×10^{-9}	4.9×10^{-10}	4.8×10^{-10}	K
Lake Kivu 2	4.5×10^{-3}	0.64	6.2	6.4×10^{-3}	8.6×10^{-3}	3.5	2.4×10^{-11}	1.6×10^{-11}	1.8×10^{-11}	L

* In Kelley (1984).
† In Fernando (1989).

Parameterization developed by Fernando (1989) has not been used here because it strongly depends on the thickness of the convective layer, which is inconsistent with the experimental observation in thermal convection (Puits et al., 2007). Among these heat flux parameterizations, Kelley (1990) formula has been most commonly used in the oceanographical community, but none of them is verified in a rigorous theoretical frame of diffusive convection. Therefore, the heat buoyancy fluxes q_{TM}, q_{TT}, and q_{TK} are all used here.

3. Data, results and discussion

3.1. Data

The observations of regular, well-formed diffusive convection staircases were collected in a wide range of conditions. These data were observed in the Arctic (Neshyba et al., 1971; Perkin and Lewis, 1984; BGOS, 2012; Zhou and Lu, 2013), Antarctica (Shirtcliffe and Calhaem, 1968; Middleton and Foster, 1980; Muench et al., 1990), Red Sea (Anschutz and Blanc, 1996; Swift et al., 2012), saline lakes (Newman, 1976; Schmid et al., 2010), and other regions (Larson and Gregg, 1983). Most publically accessible data used in previous studies (Kelley, 1984; Fernando, 1989) are included here for comparison. In most cases, the relevant quantities of diffusive convection staircases were obtained from the published profiles and tables. Some data errors are unavoidable, but we found the error of temperature difference ΔT is less than 5% and that of thickness H is less than 2%. Another possible deviation is that most published profiles are instantaneous data, which might not be representative of the average conditions. These data are summarized in Table 1, which indicates that the range of N is between 2.3×10^{-4} and $0.17\ s^{-1}$, that of q_T is between 1.0×10^{-12} and $1.6 \times 10^{-7}\ m^2\ s^{-3}$ with the estimations from Eqs. (9) and (10), and that of R_ρ is between 1.4 and 12.5.

3.2. Comparison with earlier models

Two layer thickness parameterizations are chosen to compare with the observed layer thickness H. First, Kelley's (1984) parameterization (Eq. (2)) is examined. Fig. 2a, the layer thickness H compensated by the term G_1 in Eq. (2) is plotted as a function of length scale $(\kappa_T/N)^{1/2}$. Some data collapse on the predicted curve rather well. Table 1 indicates that the buoyancy flux q_T of these data varies in a small range of 10^{-11} to $10^{-9}\ m^2\ s^{-3}$. Data in the deep Arctic and in the Red Sea largely deviate from the predictions. As listed in Table 1, q_T is about $10^{-12}\ m^2\ s^{-3}$ in the deep Arctic and $10^{-6}\ m^2\ s^{-3}$ in the Red Sea. Therefore, it is concluded that the buoyancy flux q_T is responsible for the deviation between the observations and Kelley's (1984) predictions. In other words, q_T must be included in the expression of layer thickness.

Next, the parameterization of Fernando (1989) is examined. In this parameterization (Eq. (5)), the buoyancy flux q_T of individual convecting layer must be estimated. Here, the heat flux formula of Fernando (1989) is not used because it links to the thickness H. Instead, the heat flux formula proposed by Kelley (1990) (Eqs. (9) and (10a)) is employed because it is independent of the thickness H and it has been extensively applied in the oceans and lakes. As shown in Fig. 2b, the layer thickness H compensated by the term G_3 in Eq. (5) is plotted as a function of length scale $(q_T/N_S^3)^{1/2}$. It indicates that the observed thickness H scatters, but the general trend seems reasonable. The scatter implies that the dependent scaling between H and $(q_T/N_S^3)^{1/2}$ is inappropriate, which motivated us to find another length scale in the new model.

3.3. Results of the new model

In the new model, G_4 in Eq. (7) is a function of stability ratio R_ρ and is determined by the in situ observations. As the heat related buoyancy flux q_T is estimated from three different heat flux parameterizations (Marmorino and Caldwell, 1976; Taylor, 1988; Kelley, 1990), the corresponding analysis may result in G_4 of different forms. The results based on the parameterization of Marmorino and Caldwell (1976) are plotted in Figs. 3a and b. Fig. 3a shows the normalized thickness, $H/[q_{TM}^3/(\kappa_T N^8)]^{1/4}$, as a function of R_ρ. It is indicated that the data can be well fitted by a simple function, which leads to $G_4 = 8.09(R_\rho - 1)^{2.08}$. The results based on q_{TT} (Taylor, 1988) are plotted in Fig. 3c, the fitted G_4 is slightly different, which has the form $G_4 = 13.70(R_\rho - 1)^{2.11}$. The results based on q_{TT} (Kelley, 1990) are plotted in Fig. 3e, the fitted G_4 is $G_4 = 12.78(R_\rho - 1)^{1.81}$. Successively, the dependencies of H/G_4 on H_0 obtained from q_{TM}, q_{TT}, and q_{TK} are respectively plotted in Figs. 3b, d, and f to examine whether or not $[q_{TM}^3/(\kappa_T N^8)]^{1/4}$ is the appropriate length scale. It is seen that the observational data converge toward the predicted curves respectively. Moreover, it is necessary to check the dependency of thickness H on each individual quantity. As shown in Fig. 4a, when the dependence of $H/[G_4(q_T^3/\kappa_T)^{1/4}]$ on N is fitted with the least squares method, the fitted scaling is -1.94 ± 0.10 with a correlation coefficient of 0.97, which is very close to the proposed scaling -2 in the new model. As shown in Fig. 4b, the scaling between $HN^2\kappa_T^{1/4}/G_4$ and q_T is fitted as 0.75 ± 0.03 with a correlation coefficient of 0.98, which is close to the proposed scaling 3/4 too. Compared to the previous mixed layer parameterizations shown in Fig. 2, the new one provides more accurate predictions even though there exists some uncertainties in the

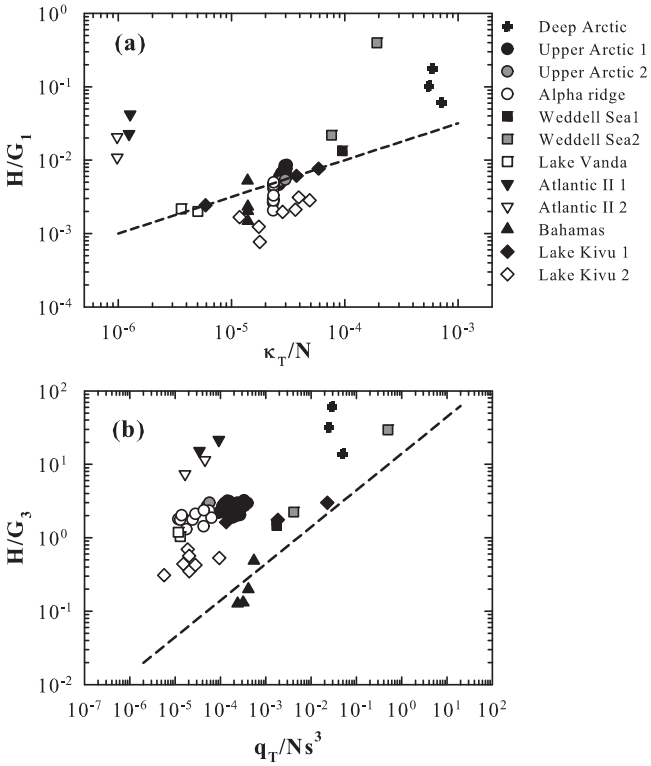

Fig. 2. (a) Dependence of the compensation of observed thickness H/G_1 on the length scale κ_T/N. G_1 is a function of Pr and R_ρ in Eq. (2) (Kelley, 1984). The prediction by Kelley (1984) is plotted as a dashed line. (b) Dependence of the compensation of observed thickness H/G_3 on the length scale q_T/N_s^3. G_3 is a function of R_ρ in Eq. (5) (Fernando, 1989). The prediction by Fernando (1989) is plotted as a dashed line. Data Sources: Deep Arctic (Zhou and Lu, 2013) – crosses; Upper Arctic 1 (BGOS, 2012) – solid circles; Upper Arctic 2 (Neshyba et al., 1971) – gray circles; Alpha ridge (Perkin and Lewis, 1984)– open circles; Weddell Sea 1 (Middleton and Foster, 1980) – solid squares; Weddell Sea 2 (Muench et al., 1990) – gray squares; Lake Vanda (Shirtcliffe and Calhaem, 1968) – open squares; Atlantic II 1 (Anschutz and Blanc, 1996) – solid down-triangles; Atlantic II 2 (Swift et al., 2012) – open down-triangles; Bahamas II (Larson and Gregg, 1983) – solid up-triangles; Lake Kivu 1 (Newman, 1976)– solid diamonds; and Lake Kivu 2 (Schmid et al., 2010) – open diamonds.

evaluation of heat related buoyancy flux q_T. To summarize, based on these results from three different heat flux parameterizations, Eqs. (9) and (10a), the corresponding layer thicknesses H in Eq. (7) are respectively predicted to be

$$H = 8.09(R_\rho - 1)^{2.08}\left(\frac{q_{TM}^3}{\kappa_T N^8}\right)^{1/4}, \tag{11a}$$

$$H = 13.70(R_\rho - 1)^{2.11}\left(\frac{q_{TT}^3}{\kappa_T N^8}\right)^{1/4}, \tag{11b}$$

and

$$H = 12.78(R_\rho - 1)^{1.81}\left(\frac{q_{TK}^3}{\kappa_T N^8}\right)^{1/4}. \tag{11c}$$

Eq. (11) shows that H has slightly different scalings of R_ρ due to the different heat flux parameterizations. As listed in Table 1, it is found that the heat-related buoyancy fluxes q_T estimated from different parameterizations are more or less consistent with each other to most of the data. Therefore, the scaling uncertainty between H and R_ρ is induced by the prediction uncertainties by different heat flux parameterizations. Eq. (11) can be alternatively generalized as

$$H \sim (R_\rho - 1)^{2.0\pm0.20}\left(\frac{q_T^3}{\kappa_T N^8}\right)^{1/4}. \tag{14}$$

Here it is indicted that H gets 0 when R_ρ approaches 1. This is consistent with the theoretical prediction that the diffusive convection becomes unstable and will disappear as the density ratio is less than or equals to 1 (Kelley et al., 2003).

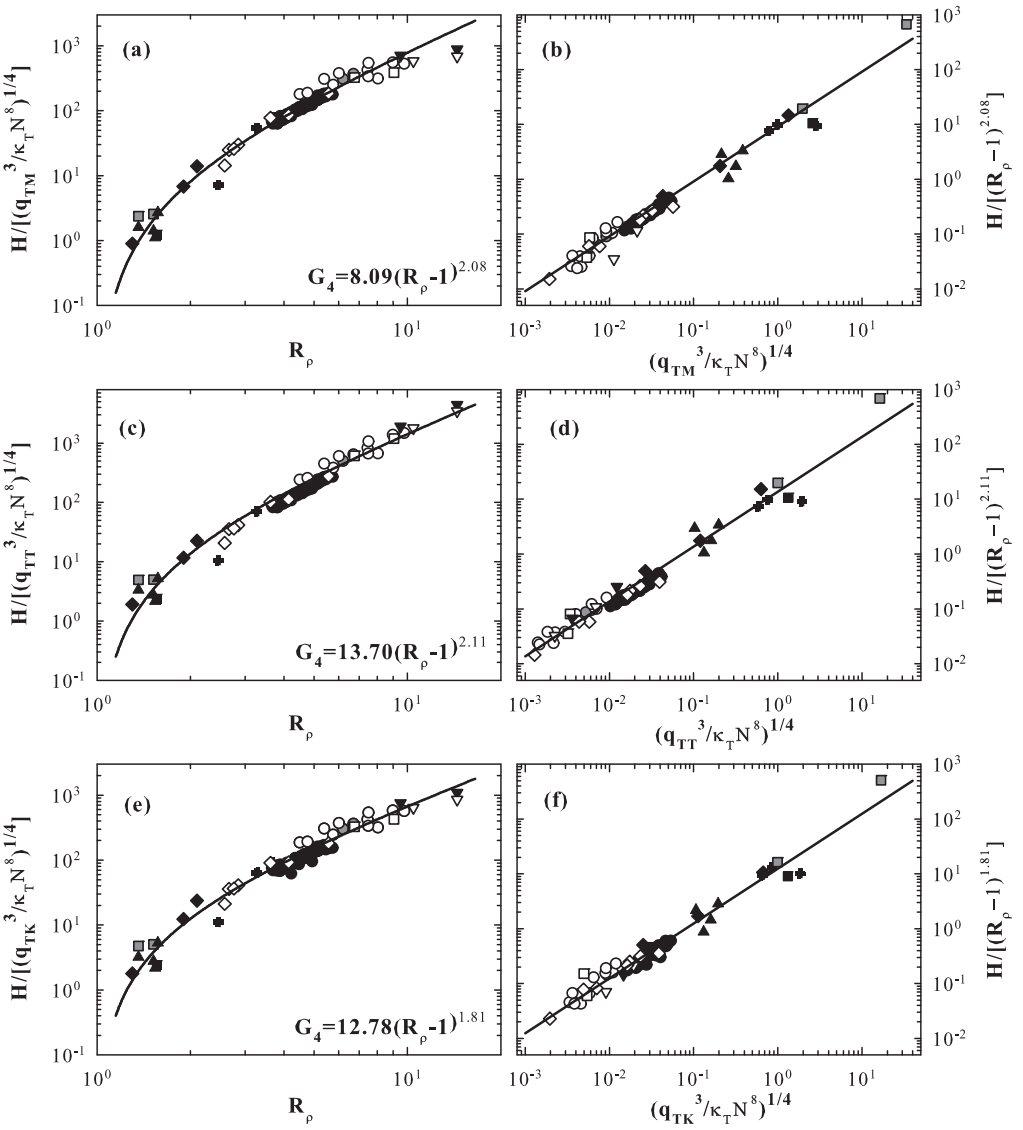

Fig. 3. (a) Dependence of the compensation of observed thickness $H/[q_{TM}^3/(\kappa_T N^8)]^{1/4}$ on the stability ratio R_ρ. q_{TM} is based on the heat flux parameterization of Marmorino and Caldwell (1976) (Eq. (7)). $G_4 = 8.09(R_\rho - 1)^{2.08}$ is plotted as a solid line. (b) Dependence of the compensation of observed thickness $H/[8.09(R_\rho - 1)^{2.08}]$ on the thickness scale $[q_{TM}^3/(\kappa_T N^8)]^{1/4}$. Equation (12a) is plotted as a solid line. (c) Dependence of $H/[q_{TT}^3/(\kappa_T N^8)]^{1/4}$ on R_ρ. q_{TT} is based on the heat flux parameterization of Taylor (1988) (Eq. (8)). $G_4 = 13.70(R_\rho - 1)^{2.11}$ is plotted as a solid line. (d) Dependence of $H/[13.70(R_\rho - 1)^{2.11}]$ on $[q_{TT}^3/(\kappa_T N^8)]^{1/4}$. Equation (12b) is plotted as a solid line. (e) Dependence of $H/[q_{TK}^3/(\kappa_T N^8)]^{1/4}$ on R_ρ. q_{TK} is based on the heat flux parameterization of Kelley (1990) (Eq. (9)). $G_4 = 12.78(R_\rho - 1)^{1.81}$ is plotted as a solid line. (f) Dependence of $H/[12.78(R_\rho - 1)^{1.81}]$ on the thickness scale $[q_{TK}^3/(\kappa_T N^8)]^{1/4}$. Equation (12c) is plotted as a solid line. The representations of data sources are the same as those in Fig. 2a.

3.4. Physics in the new model

We attempt to understand the physics represented in the new model. In the sheared stratified environments, the vertical overturn represents the large energy-containing eddies (Ozmidov, 1965). Based on the energy cascading of Kolmogorov's theory, the overturning length scale has a form of $L = \eta Re^{\gamma}$, here $\eta = (\nu^3/\epsilon)^{1/4}$ is the Kolmogorov length scale and Re is the Reynolds number (Kolmogorov, 1941). With the dimensional argument, γ is derived to be 3/4 in fully developed turbulence. A number of the overturning length scales has been defined to characterize the dynamics of turbulence. The balance between the buoyancy forces and the inertial forces is represented by the Ozmidov length scale, $L_o = (\epsilon/N^3)^{1/2}$, here ϵ is the dissipation rate, was proposed and it is often assumed to be a universal descriptor of the overturning scale (Ozmidov, 1965). Ivey et al. (2000) defined another length scale as $L_v = (\nu\epsilon)^{1/4}/N$ to be relevant to weakly energetic stratified flows. While in highly energetic flows, the overturning scale was suggested to be $L_p = (\nu/N)^{1/2}$ (Gargett, 1988; Barry et al., 2001). In the stratified fluid, the buoyancy Reynolds number $Re_b = \epsilon/(\nu N^2)$ is commonly used to represent the intensity of turbulent flow. When Re_b

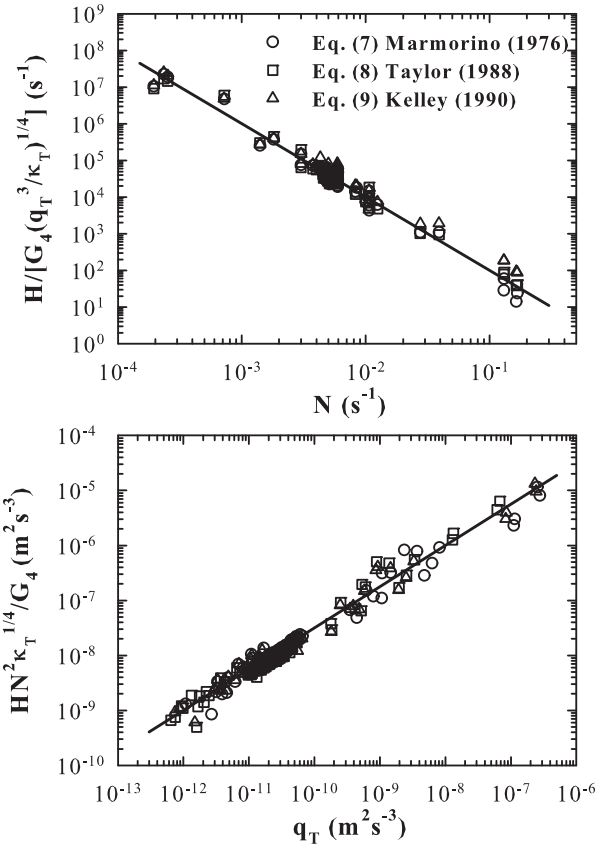

Fig. 4. (a) Dependence of the compensation of observed thickness $H/[G_4(q_T^3/\kappa_T)^{1/4}]$ on buoyancy frequency N. The best fitting is plotted as a solid line with the scaling of −1.94. (b) Dependence of the compensation of observed thickness $HN^2\kappa_T^{1/4}/G_4$ on heat-related buoyancy flux q_T. The best fitting is plotted as a solid line with the scaling of 0.75. Results obtained from the heat related buoyancy flux q_{TM} (Eq. (7)), q_{TT} (Eq. (8)), and q_{TK} (Eq. (9)) are plotted as open circles, open squares, and open triangles, respectively. The sources of data are the same as those in Fig. 2a.

is used in $L = \eta Re_b^{\gamma}$, it is found that the overturning length scale L_p, L_v, and L_o can be obtained corresponding to $\gamma = 1/4$, 1/2, and 3/4 respectively. That is, the overturning length scale L has different forms at different flow conditions.

In the double diffusive convection, the turbulent flow is not directly driven by the shear instability, and one cannot expect the scaling arguments in shear turbulence can be appropriately applied in the convective turbulence. Ruddick et al. (1997) found that the dissipation rate ϵ is almost equivalent to the buoyant flux q in the salt finger regime (St Laurent and Schmitt, 1999). When it is assumed that the heat buoyant flux q_T is comparable with the dissipation rate ϵ in the diffusive convection, the intrinsic scale H_0 of the layer thickness seems to be related to these overturning length scales. In the earlier models, $H_0 = (\kappa_T/N)^{1/2}$ in the formula of Kelley (1984) can be written as $H_0 = L_p/Pr^{1/2} = \eta Re_b^{1/4}/Pr^{1/2}$, while $H_0 = (q_T/N^3)^{1/2}$ in that of Fernando (1989) is $H_0 = L_o = \eta Re_b^{3/4}$. According to this argument, it seems that H_o can be regarded as the length scale of an energy-containing eddy too. However, as shown in Fig. 2, the H_0 representations in the earlier models cannot be applied to the diffusive condition in the wide condition range. In the new model, the intrinsic length $H_0 = [q_T^3/(\kappa_T N^8)]^{1/4}$ also has a simple form that can be written as $H_0 = \eta Re_b Pr^{1/4}$. Although it cannot connected with the available overturning length scale in the sheared stratified turbulence, as shown in Figs. 3 and 4, this scale is the best descriptor of the thickness scale of turbulence for diffusive convection. In other words, $H_0 = \eta Re_b Pr^{1/4}$ provides another overturning length scale, which should be considered in the turbulent flow of double diffusive convection.

The new model can be further understood by examining each quantity in Eq. (14). As q_T is the heat-related buoyancy flux across the convecting layer, larger q_T can lead to the stronger coherent structures (plumes or thermals), as observed in the Rayleigh–Bérnard convection (Zhou and Xia, 2002). These stronger structures would have more potential to thicken the convecting layer. This is consistent with the relation of $H \sim q_T^{3/4}$ in Eq. (14). N reflects the background stratification. As proposed in linear stability analysis (Turner, 1973), stable stratification inhibits the onset of convective instability. Therefore, it is apprehensible that $H \sim 1/N^2$ in the new model. R_ρ reflects the competition between the stabilizing and destabilizing effects. It is difficult to offer a reasonable explanation for the dependence of H on R_ρ ($H \sim (R_\rho - 1)^2$) in the new model. When comparing Eqs. (6) with (14), it seems that R_ρ in Eq. (14) plays the same role as Ra_c in Eq. (6). As discussed in Turner (1973), Ra_c in the diffusive convection is different from the typical value (∼1000) in the thermal convection. This is confirmed in the

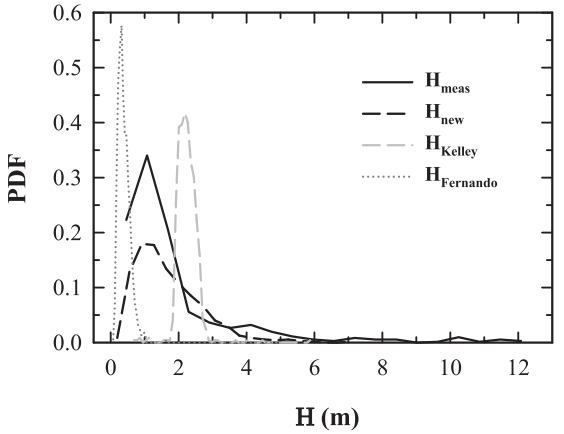

Fig. 5. The PDFs of the measured DC layer thickness (H_{meas}) in the Amundsen Basin (black solid curve). The predicted DC layer thickness from the present model (H_{new}), Kelley (1984)'s (H_{Kelley}) and Fernando (1989)'s ($H_{Fernando}$) formula is respectively plotted as black dash, gray dash and gray dotted curves.

recent work, where Ra_c can reach 10^{11} depending on the local environment conditions (Zhou et al., 2014). In some sense, the new model (Eq. (14)) is a generalized representation of the convecting layer thickness and Eq. (6) from Turner (1968) can be taken as its special case for the bottom one. Upon the discussion of the bottom convecting layer, Turner (1968) suggested that this layer reaches its maximum thickness when the advancing boundary layer becomes unstable, and then be broken down to form a secondary convecting layer. Accordingly, it is expected that the dominating mechanism proposed by Turner (1968) can be applied to other convecting layers too. In each convecting layer, the layer thickness H is strongly related to the thermodynamic process of its thermal boundary layer. H reaches a stable value when the thermal boundary layer forms a new convecting layer triggered by thermal instability. The process dominated by the convective instability mechanism, not the other mechanisms (Kelley, 1984; Fernando, 1987), is mainly responsible for the stable thickness of a convecting layer.

3.5. Application of the new model

The expression of new model (Eq. (14)) is obtained based on the empirical formulas of heat flux (Eqs. (9) and (10a)). We would examine its applicability by using the other heat flux estimation totally different from Eqs. (9) and (10a). In the diffusive convection, it is generally assumed that the molecular diffusivity plays a dominating role in the heat transfer through the laminar interface (Newell, 1984; Kelley, 1990), which can be approximated as

$$F_{mol} = \rho c_p \kappa_T \left(\frac{\partial T}{\partial z} \right)_{\max}, \tag{15}$$

where z is depth (positive downward), and $(\partial T/\partial z)_{max}$ is the maximum temperature gradient inside the interface, as shown in Fig. 1b. In principle, F_{mol} through each interface can be used to represent the heat flux through the staircase because the heat is transferred successively.

Here we use the high resolution hydrographical data measured by a microstructure profiler in the Amundsen Basin. A detailed description of these data can be found in (Sirevaag and Fer, 2012). Briefly, the data were collected between 18 and 25 April 2008 as an ice floe drifted from (88.4 N, 7.7 E) to (88.0 N, 5.3 W). The conductivity, temperature, depth were sampled at 1024 Hz and were averaged to 256 Hz to reduce noise. The falling speed of the instrument was 0.6 ms^{-1}, which corresponds to the vertical resolution of 2.5 mm; however, the time response and smoothing by the thermistor leads to an effective vertical resolution of approximately 2 cm. Of the total 213 profiles we use 169 profiles which covered the entire vertical extent of the staircase. The persistent DC staircases were observed in the depth range 200–260 m, as shown in Fig. 1a. The layer thickness is of the order of 1 m. In total, 717 staircases were collected for statistical analysis. Probability distribution function (PDF) of the measured layer thickness, H_{meas}, is shown in Fig. 5. H_{meas} varies from 0.5 to 14 m with the median value of 1.26 m, which is consistent with the value in (Sirevaag and Fer, 2012). The layer thicknesses predicted from the new model (Eq. (14)), H_{new}, and the earlier models are also shown in Fig. 5 for comparison. Note that q_T is obtained from Eq. (15) with the temperature gradient $(\partial T/\partial z)_{max}$ determined over a depth range of 2.5 cm (Fig. 1b). Fig. 5 indicates that H_{new} largely overlaps with H_{meas} with the median of 1.45 m. There are discrepancies between the predictions from Kelley (1984) and Fernando (1989)'s formula with the measured layer thickness, the median values of which are respectively 2.22 and 0.36 m.

4. Conclusions

In summary, a new parameterization is proposed to predict the convecting layer thickness H in diffusive convection. In this parameterization, the layer thickness is expected to be affected by the background stratification (N), the heat buoyant flux

through individual layer (q_T), the competition between the salinity restoring force and the thermal buoyancy (R_ρ), and fluid properties, which promote us to construct an intrinsic thickness scale H_0 ($H_0 = [q_T^3/(\kappa_T N^8)]^{1/4}$). Based on the dimensional argument, H_0 can be regarded as the scale of an energy-containing eddy and it is alternatively represented as $H_0 = \eta Re_b Pr^{1/4}$. By using in situ observations under a wide range of conditions in oceans and lakes, where the buoyancy frequency N varies between 10^{-4} and $0.1\ s^{-1}$ and the heat buoyancy flux q_T varies between 10^{-12} and $10^{-7}\ m^2\ s^{-3}$, it is found that the layer thickness H depends on the stability ratio R_ρ and the intrinsic thickness scale H_0 with the form of $H \sim (R_\rho - 1)^2 H_0$. In the laboratory work of Turner (1968), he proposed that the bottom convecting layer reach its stable thickness when its top boundary develops to be a new convecting layer. This convective instability mechanism can be used to explain the thickness of other convecting layers. To each convecting layer, its thermal boundary layer is trigged to be a new secondary convecting layer, this thermodynamic process stops the growth of the original convecting layer and makes it keep a stable thickness. It is expected that the new model should be a generalized representation of the convecting layer thickness and it can be applied in an even wider range of conditions, such as the evolution of diffusive convection in massive stars (Merryfield, 1995) and giant planets (Chabrier and Baraffe, 2007).

Acknowledgements

We thank Mary-Louise Timmermans for the constructive communication about the data in the deep Arctic Ocean, and thank Martin Schmid for sending the raw data of Lake Kivu. We also thank the anonymous reviewers for their very constructive and valuable comments. This work was supported by China NSF grants (41176027, 41476167 and 41406035), and the Strategic Priority Research Program of the Chinese Academy of Sciences (XDA11030302). Some data were collected and made available by the Beaufort Gyre Exploration Program based at the Woods Hole Oceanographic Institution (http://www.whoi.edu/beaufortgyre) in collaboration with researchers from Fisheries and Oceans Canada at the Institute of Ocean Sciences.

References

Anschutz, P., Blanc, G., 1996. Heat and salt fluxes in the Atlantis II Deep (red sea). Earth Planet. Sci. Lett. 142, 147–159, http://dx.doi.org/10.1016/0012-821X(96)00098-2.
Barry, M.E., Ivey, G.N., Winters, K.B., Imberger, J., 2001. Measurements of diapycnal diffusivities in stratified fluids. J. Fluid. Mech. 442, 267–291, http://dx.doi.org/10.1017/S0022112001005080.
BGOS, 2012. The Hydrographic Data Measured by the Ice-Tethered Profiler 2 (ITP2) in Beaufort Gyre Observing System (BGOS) were Used in the Present Work. http://www.whoi.edu/itp.
Brown, E., Nikolaenko, A., Funfschilling, D., Ahlers, G., 2005. Heat transport in turbulent Rayleigh–Bénard convection: effect of finite top- and bottom-plate conductivities. Phys. Fluids 17, http://dx.doi.org/10.1063/1.1964987, 075 108.
Chabrier, G., Baraffe, I., 2007. Heat transport in giant (exo)planets: a new perspective. Astrophys. J. Lett. 661, 81–84, http://dx.doi.org/10.1086/518473.
Chandrasekhar, S., 1961. Hydrodynamic and Hydromagnetic Stability. Clarendon Press, Oxford, 652 pp.
Fedorov, K.N., 1988. Layer thicknesses and effective diffusivities in diffusive thermohaline convection in the ocean. In: Nihoul, J.C.J., Jamart, B.M. (Eds.), Small-Scale Turbulence and Mixing in the Ocean. Elsevier, New York, pp. 471–479.
Fernando, H.J.S., 1987. The formation of layered structure when a stable salinity gradient is heated from below. J. Fluid. Mech. 182, 525–541, http://dx.doi.org/10.1017/S0022112087002441.
Fernando, H.J.S., 1989. Oceanographic implications of laboratory experiments on diffusive interfaces. J. Phys. Oceanogr. 19, 1707–1715, doi:10.1175/1520-0485(1989)019<1707:OIOLEO>2.0.CO;2.
Gargett, A.E., 1988. The scaling of turbulence in the presence of stable stratification. J. Geophys. Res. 93 (C5), 5021–5036, http://dx.doi.org/10.1029/JC093iC05p05021.
Guthrie, J.D., Fer, I., Morison, J., 2015. Observational validation of the diffusive convection flux laws in the Amundsen Basin, Arctic Ocean. J. Geophys. Res. Oceans 120, 7880–7896, http://dx.doi.org/10.1002/2015JC010884.
He, X., Funfschilling, D., Nobach, H., Bodenschatz, E., Ahlers, G., 2012. Transition to the ultimate state of turbulent Rayleigh–Bénard convection. Phys. Rev. Lett. 108, http://dx.doi.org/10.1103/PhysRevLett.108.024502, 024 502.
Huppert, H.E., Linden, P.F., 1979. On heating a stable salinity gradient from below. J. Fluid Mech. 95, 431–464, http://dx.doi.org/10.1017/S0022112079001543.
Ivey, G., Winters, K., De Silva, I., 2000. Turbulent mixing in a sloping benthic boundary layer energized by internal waves. J. Fluid Mech. 418, 59–76, http://dx.doi.org/10.1017/S0022112000008788.
Kelley, D., 1984. Effective diffusivities within oceanic thermohaline staircases. J. Geophys. Res. 89, 10484–10488, http://dx.doi.org/10.1029/JC089iC06p10484.
Kelley, D.E., 1990. Fluxes through diffusive staircases: a new formulation. J. Geophys. Res. 95, 3365–3371, http://dx.doi.org/10.1029/JC095iC03p03365.
Kelley, D.E., Fernando, H.J.S., Gargett, A.E., Tanny, J., Özsoy, E., 2003. The diffusive regime of double diffusive convection. Progr. Oceanogr. 56, 461–481, http://dx.doi.org/10.1016/S0079-6611(03)00026-0.
Kerpel, J., Tanny, J., Tsinober, A., 1991. On a stable solute gradient heated from below with prescribed temperature. J. Fluid Mech. 223, 83–91, http://dx.doi.org/10.1017/S0022112091001349.
Kolmogorov, A.N., 1941. The local structure of turbulence in incompressible viscous fluid for very large Reynolds numbers. Dokl. Akad. Nauk SSSR 30, 299–303.
Langlois, W.E., 1985. Buoyancy-driven flows in crystal-growth melts. Ann. Rev. Fluid Mech. 17, 191, http://dx.doi.org/10.1146/annurev.fl.17.010185.001203.
Larson, N.G., Gregg, M.C., 1983. Turbulent dissipation and shear in thermohaline intrusions. Nature 306, 26–32, http://dx.doi.org/10.1038/306026a0.
Marmorino, D.R., Caldwell, G.O., 1976. Heat and salt transport through a diffusive thermohaline interface. Deep Sea Res. 23, 59–67, http://dx.doi.org/10.1016/0011-7471(76)90808-1.
Merryfield, W.J., 1995. Hydrodynamics of semiconvection. Astrophys. J. 444, 318–337, http://dx.doi.org/10.1086/175607.
Middleton, J.H., Foster, T.D., 1980. Fine-structure measurements in a temperature-compensated halocline. J. Geophys. Res. 85 (C2), 1107–1122, http://dx.doi.org/10.1029/JC085iC02p01107.
Muench, R.D., Fernando, H.J.S., Stegen, G.R., 1990. Temperature and salinity staircases in the northwestern weddell sea. J. Phys. Oceanogr. 20 (2), 295–306, doi:10.1175/1520-0485(1990)020<0295:TASSIT>2.0.CO;2.

Neshyba, S., Neal, V.T., Denner, W., 1971. Temperature and conductivity measurements under ice island $t-3$. J. Geophys. Res. 76 (33), 8107–8120, http://dx.doi.org/10.1029/JC076i033p08107.
Newell, T., 1984. Characteristics of double-diffusive interface at high density stability ratios. J. Fluid Mech. 149, 385–401, http://dx.doi.org/10.1017/S0022112084002718.
Newman, F.C., 1976. Temperature steps in lake kivu. a bottom heated saline lake. J. Phys. Oceanogr. 6 (2), 157–163, doi:10.1175/1520-0485(1976)006<0157:TSILKA>2.0.CO;2.
Nikolaenko, A., Brown, E., Funfschilling, D., Ahlers, G., 2005. Heat transport by turbulent Rayleigh–Bénard convection in cylindrical cells with aspect ratio one and less. J. Fluid. Mech. 523, 251–260, http://dx.doi.org/10.1017/S0022112004002289.
Ozmidov, R., 1965. On the turbulent exchange in a stably stratified ocean. Izv. Acad. Sci. USSR, Atmos. Oceanic Phys. 1, 861–871.
Perkin, R.G., Lewis, E.L., 1984. Mixing in the west spitsbergen current. J. Phys. Oceanogr. 14 (8), 1315–1325, doi:10.1175/1520-0485(1984)014<1315:MITWSC>2.0.CO;2.
Puits, R.D., Resagk, C., Tilgner, A., Busse, F.H., Thess, A., 2007. Structure of thermal boundary layers in turbulent Rayleigh–Bénard convection. J. Fluid. Mech. 572, 231–254, http://dx.doi.org/10.1017/S0022112006003569.
Robb, L., 2004. Introduction to Ore-forming Processes. Blackwell Publishing, pp. 373pp.
Rohden, C.V., Boehrer, B., Ilmberger, J., 2010. Evidence for double diffusion in temperate meromictic lakes. Hydrol. Earth Syst. Sci. 14, 667–674, http://dx.doi.org/10.5194/hess-14-667-2010.
Ruddick, B., Walsh, D., Oakey, N., 1997. Variations in apparent mixing efficiency in the north atlantic central water. J. Phys. Oceanogr. 27 (12), 2589–2605, doi:10.1175/1520-0485(1997)027<2589:VIAMEI>2.0.CO;2.
Schmid, M., Busbridge, M., Wüest, A., 2010. Double diffusive convection in Lake Kivu. Limnol. Oceanogr. 55, 225–238, http://dx.doi.org/10.4319/lo.2010.55.1.0225.
Schmitt, R.W., 1994. Double diffusion in oceanography. Annu. Rev. Fluid Mech. 26, 255–285, http://dx.doi.org/10.1146/annurev.fl.26.010194.001351.
Schmitt, R.W., Ledwell, J.R., Montgomery, E.T., Polzin, K.L., Toole, J.M., 2005. Enhanced diapycnal mixing by salt fingers in the thermocline of the tropical atlantic. Science 308 (5722), 685–688, http://dx.doi.org/10.1126/science.1108678.
Shirtcliffe, T.G.L., Calhaem, I.M., 1968. Measurements of temperature and electrical conductivity in lake vanda, victoria land, antarctica. NZ J. Geol. Geophys. 11 (4), 976–981, http://dx.doi.org/10.1080/00288306.1968.10420763.
Siggia, E.B., 1994. High Rayleigh number convection. Annu. Rev. Fluid Mech. 26, 137–168, http://dx.doi.org/10.1146/annurev.fl.26.010194.001033.
Sirevaag, A., Fer, I., 2012. Vertical heat transfer in the Arctic Ocean: the role of double-diffusive mixing. J. Geophys. Res. 117, C07 010, doi:10.1029/2012JC007910.
St. Laurent, L., Schmitt, R.W., 1999. The contribution of salt fingers to vertical mixing in the north Atlantic tracer release experiment. J. Phys. Oceanogr. 29 (7), 1404–1424, doi:10.1175/1520-0485(1999)029<1404:TCOSFT>2.0.CO;2.
Swift, S.A., Bower, A.S., Schmitt, R.W., 2012. Vertical, horizontal, and temporal changes in temperature in the Atlantis II and discovery hot brine pools, red sea. Deep Sea Res. I 64, 118–128, http://dx.doi.org/10.1016/j.dsr.2012.02.006.
Taylor, J., 1988. The fluxes across a diffusive interface at low values of the density ratio. Deep Sea Res. I 35, 555–567, http://dx.doi.org/10.1016/0198-0149(88)90131-8.
Timmermans, M.L., Garrett, C., Carmack, E., 2003. The thermohaline structure and evolution of the deep waters in the Canada Basin. Arctic Ocean. Deep Sea Res. I 50, 1305–1321, http://dx.doi.org/10.1016/S0967-0637(03)00125-0.
Turner, J.S., 1968. The behavior of a stable salinity gradient heated from below. J. Fluid Mech. 33, 183–200, http://dx.doi.org/10.1017/S0022112068002442.
Turner, J.S., 1973. Buoyancy Effects in Fluids. Cambridge University Press, 367 pp.
Turner, J.S., 2010. The melting of ice in the arctic ocean: the influence of double-diffusive transport of heat from below. J. Phys. Oceanogr. 40, 249–256, http://dx.doi.org/10.1175/2009JPO4279.1.
Wong, A.P., Riser, S.C., 2011. Profiling float observations of the upper ocean under sea ice off the Wilkes land coast of Antarctica. J. Phys. Oceanogr. 41, 1102–1115, http://dx.doi.org/10.1175/2011JPO4516.1.
You, Y.Z., 2002. A global ocean climatological atlas of the turner angle: implications for double-diffusion and water-mass structure. Deep Sea Res. I 49, 2075–2093, http://dx.doi.org/10.1016/S0967-0637(02)00099-7.
Zhang, J., Schmitt, R.W., Huang, R.X., 1999. The relative influence of diapycnal mixing and hydrologic forcing on the stability of the thermohaline circulation. J. Phys. Oceanogr. 29, 1096–1108, doi:10.1175/1520-0485(1998)028<0589:SOTGMO>2.0.CO;2.
Zhou, S.-Q., Lu, Y.-Z., 2013. Characterizations of double diffusive convection steps and heat budget in the deep arctic ocean. J. Geophys. Res. (in revision).
Zhou, S.-Q., Qu, L., Lu, Y.-Z., Song, X.-L., 2014. The instability of diffusive convection and its implication for the thermohaline staircases in the deep arctic ocean. Ocean Sci. 10 (1), 127–134, http://dx.doi.org/10.5194/os-10-127-2014.
Zhou, S.-Q., Xia, K.-Q., 2002. Plumes statistics in thermal turbulence – the mixing of an active scalar. Phys. Rev. Lett. 89, http://dx.doi.org/10.1103/PhysRevLett.89.184502, 184 502.